

# Knowledge-rich optimisation of prefabricated façades to support conceptual design

Jacopo Montali\*, Glass and Façade Technology Research Group, University of Cambridge, Trumpington Street, CB2 1PZ, United Kingdom

Michele Sauchelli, formerly Engineering Excellence Group, Laing O'Rourke plc, Bridge Place, 1-2 Anchor Blvd, Crossways, Dartford DA2 6SN, United Kingdom

Qian Jin, College of Architecture and Urban Planning, Tongji University, 1239 Siping Road, Shanghai, 200092, China

Mauro Overend, Glass and Façade Technology Research Group, University of Cambridge, Trumpington Street, CB2 1PZ, United Kingdom

\*corresponding author

## Abstract

One of the principal challenges in façade design is to support the architectural intent by devising technically viable (i.e. standard-compliant and manufacturable) solutions from as early as possible in the design stage. This is increasingly relevant as prefabricated façades increase in complexity and bespoke-ness in response to current societal, financial and environmental challenges. In this paper a process that addresses this challenge is presented. The process consists of two sub-processes 1) to build product-oriented knowledge bases and digital tools for supporting design on a project-by-project basis and 2) to help designers identify a set of optimal solutions that consider the façade-specific trade-off between architectural intent and performance requirements, while meeting the largest number of production-related constraints. This process was applied to a case study and the results were compared with those obtained from a recently-developed façade. It was found that, although the proposed process produces optimal solutions that are approximated, designers can benefit from more control over the product's manufacturability, performance and architectural intent in less time.

## Keywords

Facade design, design optimisation, knowledge-based approaches, design for manufacture and assembly

## Nomenclature

BPBN	Business Process Modelling and Notation
CF	Constraint Function
DFMA	Design for Manufacture and Assembly
GA	Genetic Algorithm
KB	Knowledge Base

34	MOKA	Methodology and tools Oriented to Knowledge-Based Engineering Applications
35	PM	Product Model
36	UML	Unified Modelling Language
37	WCS	Weighted Constraint Score

## 38 **1 Introduction**

39 In the last two decades the construction sector has experienced increasing demands to deliver high  
40 performance and complex buildings while ensuring cost efficiency, quality and reduced delivery times  
41 [1,2]. These challenges have been addressed by new higher performance products and systems that  
42 meet the increasingly stringent regulations and standards. However, this approach has resulted in an  
43 increasingly complex building procurement and building design process, to the extent that the final  
44 product performance is not known accurately, thus increasing the chance of incurring into unforeseen  
45 errors during the construction stage [3]. In addition, productivity improvements in the construction  
46 sector are not keeping pace with those of other industries, such as manufacturing [4]. Off-site  
47 manufacture is considered essential for targeting the above challenges [5,6], but this requires early  
48 design and planning, although early commitment to manufacturer-specific systems by clients and  
49 designers is often seen as a limitation to the architectural expression. Therefore, design solutions  
50 should consider a multitude of performance and constructability criteria, as well as standard  
51 compliance, while remaining sufficiently generic to be “tenderable” by multiple contractors. In this  
52 way, competition between bidders remains high, so that quality and cost-effectiveness are achieved.  
53 Optimisation procedures can help designers understand the benefits of manufacturer-specific product  
54 integration into their design, but real-world applications are still lacking [7].

55 Façades play a fundamental role in buildings: they act as technological, multipurpose filters between  
56 the inner and the outer environment. They significantly affect the overall embodied and operational  
57 carbon emissions as well as the internal comfort levels of buildings. Façades can constitute up to the  
58 30% of the overall building construction cost [8]. If prefabricated, they are more similar to industrial  
59 products and as such, they require production-related constraints to be considered [9]: a design for  
60 Manufacture and Assembly approach [10] would thus be beneficial particularly during early stages,  
61 which are known to have disproportionally large impact on the final cost of the system. Façades also  
62 provide that aesthetic expression to the building which makes cities more habitable and pleasant to  
63 live in. This two-folded nature of designing façades, as both technical and aesthetical artefacts, is  
64 seldom acknowledged by the multitude of stakeholders involved in the design and construction  
65 process, which rather prefer to act as single entities driven by their own responsibility, views and  
66 interests.

67 Facade design is nowadays seen as an increasingly complex activity. Potential failure mechanisms  
68 across multiple domains require many experts to perform detailed analyses and, at the same time,  
69 the multitude of performance requirements needs to be managed and understood by the architect,  
70 to then support the architectural intent while introducing systems from specific manufacturers into  
71 their design. Ideally, the architect would design the facade in such a way that specialists (e.g. façade  
72 consultants, building physicists, fire / acoustic / structural engineers) or system suppliers do not have  
73 to propose substantial changes to the solution, but only to perform detailed analyses to add further

levels of detail and to confirm that the original design complies with performance requirements and manufacturing limits. Downstream knowledge (i.e. manufacturing) would thus be brought upstream in the process (i.e. conceptual stage). In this way, there would be no significant modification to the original design due to the reduction in design iterations between specialists. In this ideal world, there would be a clear-cut between the aesthetic design and the engineering analysis of the facade product [11]; those two phases would take place subsequently in time, one after the other, with no need to back cycle.

The reality of facade design differs from that ideal in that consultants propose design changes and designers modify the final design accordingly, thus requiring the work of the consultant who came chronologically before to be repeated (Figure 1). It is an iterative, interdependent and ill-structured activity and it differs from other design activities in that the supply chain is large and the design is driven by the aesthetical appearance. The influence of energy regulations on architectural design also leads to additional design loops. Moreover, the more complex (i.e. lower standardisation) the project, the higher the need to increase design iterations. The absence of certain actors in the design process (e.g. façade subcontractors), especially during early stages, constitutes an additional limit. Rules-of-thumb and design guidelines, in the form of reports / datasheets, appear to be a valuable resource in this sense, since the architect can take quick actions to get closer to the final, standard- and specification-compliant, design solution. However, the integration of design criteria still appears to be fragmented [3,8].

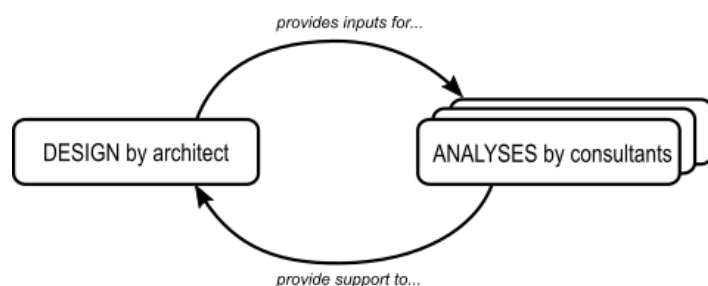


*Figure 1: Façade design is a back-and-forth activity between design and analysis of the system to be designed.*

Automation of repetitive design tasks and digitalisation of knowledge is a possible route towards the improvement of how façades are designed. The main potential benefits are the reduction of the number of iterations in Figure 1, thus resulting in increased design efficiency and more optimised solutions. Automation, and subsequent optimisation, of design tasks in façade design require the use of knowledge management techniques, as well as the development of specific optimisation procedures.

In the facade sector, there is little literature available on the link between facade products and the underlying design knowledge [12], especially in a Design for Manufacture and Assembly (DFMA [10]) perspective. So-called “façade design manuals” (e.g. [13]) cover the whole performance spectrum and basic construction technologies, but they lack insight on specific products manufactured by specific companies. Klein [8] provided a methodology to map the hierarchical structure of the facades’ physical components to both their functions and their interface types, based on Ulrich’s [14] definition of product architecture. Conversely, catalogues and manuals from real-world system/product suppliers do not focus on design principles and are organised in an independent, unstructured, way. Suppliers have produced their own catalogues, normally in the form of PDF documents, and they partially hold

production-specific knowledge, which is seldom digitalised and is normally communicated via phone calls after specific enquiries from designers or façade consultants [9].

Digitalisation and automation of knowledge is scarce. Karhu [15] built a Product Model of precast concrete facades by defining the product taxonomy and the related information. Recently, some efforts have been made to develop specific digital tools supporting specific facade products [16–18]. Semantic enrichment of the Industry Foundation Classes (IFC) schema [19] and rule-checking of Building Information Modelling [20] are the currently-pursued approaches.

Computational optimisation of facades design is instead rich and widely analysed in the academy, especially for whole life energy/cost calculations [21–23], optimal control of active facades [24–27] or panelization/form finding of complex geometries [28–30]. Genetic Algorithm (GA) is largely used to identify optimal solutions in a computationally-efficient manner. However, the extensive use of these approaches on real-world projects is still limited [7]. Moreover, the above-mentioned optimisation applications normally focus on finding one or more exact solutions for a problem defined by limited number of simplified constraints. This evidence contrasts with the requirements of façade design, which ought to consider concurrently the largest spectrum of design and manufacturing criteria.

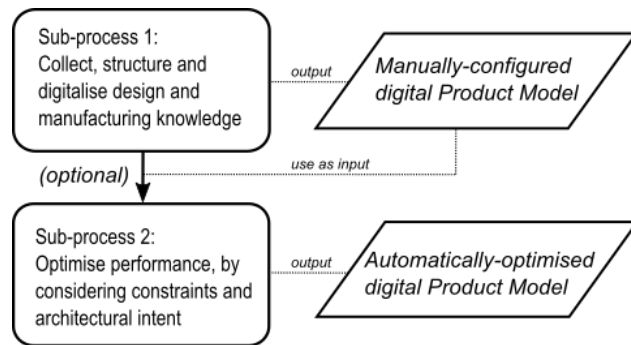


Figure 2: Flowchart of the present paper: first digitalise knowledge-based rules and constraints for configuration, then optimise (optional).

The main motivations for the present work are the need for properly-constrained optimisation approaches that consider the architect's role and the absence of techniques for the automation of design knowledge in the façade sector (Figure 2). To this end, we introduce a two-step process formed of two consecutive sub-processes: one to build DFMA-oriented and product-based knowledge bases and the corresponding digital tool (Section 2.1), and another one that optimises façades as products with some aesthetics expression, products that require specific performances, and products that need to be manufactured and installed (Section 2.2). In Section 3 we apply both sub-processes to a real-world residential project in London and their opportunities and limitations are highlighted. Sections 4 and 0 conclude with a discussion and insights on future work.

## 2 Methodology

### 2.1 Sub-process 1: the creation of the Knowledge Base (KB) and the digital tool

The creation of the knowledge-based digital tool follows what described in Montali et al. [31] (Figure 3). It is a product-based approach, in which the study of the product architecture is central through

the creation of the so-called Product Model (PM), a network of interrelated concepts that include physical features of the product, as well as the underlying design and manufacture knowledge. The sub-process consists of four main steps: 1) knowledge collection, 2) creation of the Knowledge Base representing the PM, 3) UML diagramming of the PM and 4) implementation of the PM into the digital tool. Steps 1), 3) and 4) are discussed in [31], whereas the second step is explored further in the present paper with regards to the definition of “product architecture” as per Ulrich [14] and as applied by Klein [8] to façade systems. So-called “ICARE” forms, from the MOKA [32] methodology are used to store and structure the collected knowledge. The following sub-steps<sup>1</sup> from step 2) can be identified (Figure 3 and Figure 4).

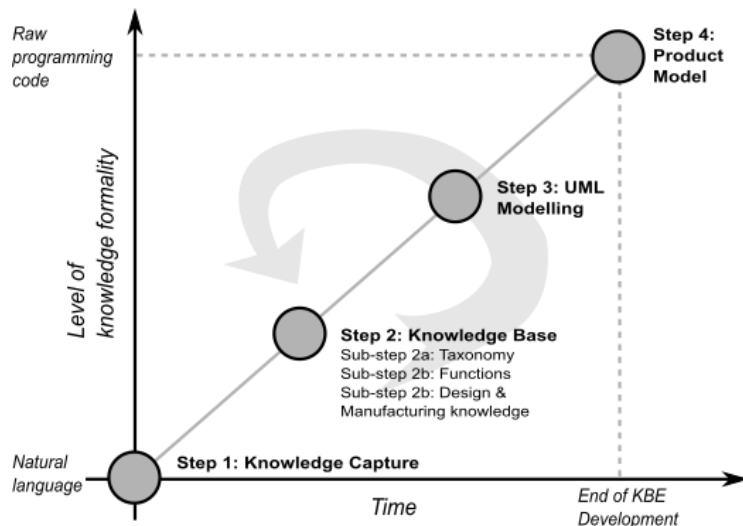


Figure 3: Sub-process 1 to build the digital tools for supporting façade design (extended from [31]).

### 2.1.1 Sub-step 2a: define the product taxonomy

This step involves the analysis of the product’s physical components and their part-whole relationship, thus leading to the definition of the product taxonomy (or “product breakdown”). For example, if we consider the “unitised façade system” as the overarching product, its subcomponents will be the structural profiles, the infill panels (glazed or opaque), the connections with the primary structure and the gaskets or seals. The components are represented by blue squares (Figure 4), and the continuous line that connects them represents the part-whole relationship (aka “contains” relationship). The component positioned above a generic component represents the “whole”, whereas elements located below it represent its “parts”.

The relevant MOKA forms (“Entity-Structure” form) representing the physical entities are then created based on the taxonomy and stored in the Knowledge Base. The part-whole relationship is expressed through links (e.g.: hypertext) placed in the appropriate form field.

### 2.1.2 Sub-step 2b: associate the product’s functions with the taxonomy

The creation of the product taxonomy is then followed by the connection between the functions and each physical component. Once the functions of the product have been specified, they are associated with the corresponding physical components. Following the example above, the “connect to primary

<sup>1</sup> Steps a) and b) correspond to steps 4) and 3) in Klein [8], respectively. The functions are selected from the “function tree” and linked to the product’s taxonomy. The taxonomy is built in turn from the “product levels”. Step c) extends Klein’s work.

structure” function will be linked to the connection between the panel and the structural slab, whereas both the “provide thermal insulation” and “withstand wind loads” functions will be associated with the structural profiles and the infill panels. Figure 4 shows the functions as orange rhombuses, and the connections to the physical components (blue squares) represent the link between the physical components and their functions.

The functions are stored in the KB by creating “Entity-Function” forms and by linking each function to a specific physical entity from the previously-created “Entity Structure” forms.

### 2.1.3 Sub-step 2c: associate design knowledge with the taxonomy

In this step the design and manufacturing knowledge collected in step 1 (knowledge collection) is associated with a specific physical element. In the above example of the unitised system, a “maximum glazed element dimensions” (e.g. obtained after specific enquiry to a glass supplier) constraint that defines the maximum width and height of a specific glass infill panel will be associated with the manufacturing constraints of glazing units. In Figure 4 these elements are represented by green circles and they are linked to physical components (blue squares). The link represents the association between a design criterion (rule, constraint) and the corresponding physical component.

The design and manufacturing rules/constraints are included in the KB by creating the MOKA forms for Rules, Constraints, Activities and Illustrations for each unit of knowledge collected and by linking the forms to the relevant “Entity-Structure” forms representing the physical components. The MOKA form can include the original knowledge source, if necessary (e.g.: contact person, document reference, etc..).

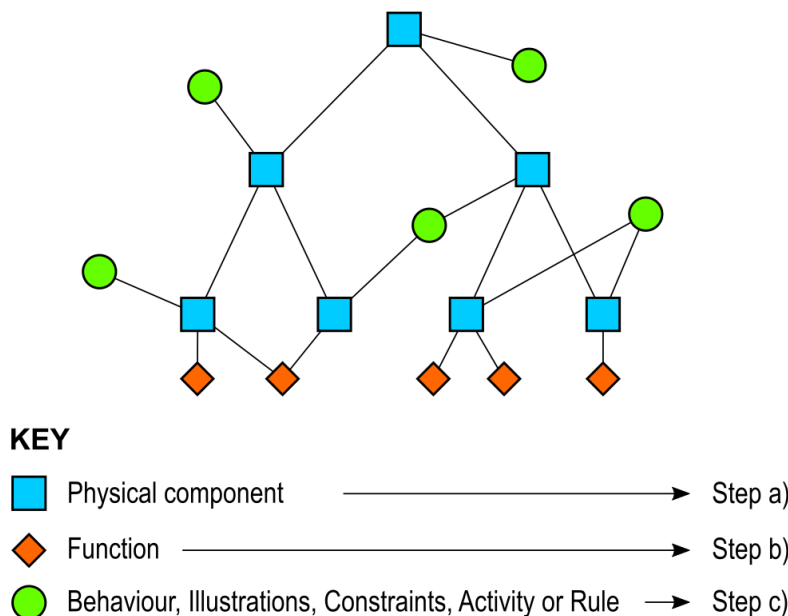


Figure 4: Graphical representation of the three sub-steps to build the knowledge base.

## 2.2 Sub-process 2: determination of the set of optimal solutions

Multi-objective optimisation is here built to determine the optimal trade-off between 1) the architectural intent and 2) the required performance, while taking into account a series of 3) constraints. The three elements are explored in a so-called “meta-domain” and they are represented

by a scatterplot (Figure 5b). The idea is to generate a relatively large number of solutions starting from the solution initially conceived through the knowledge-based tool (here defined as “proposed design”) and to explore the optimal ones by applying small variations from the proposed design.

The X-axis in Figure 5 represents the architectural intent, which is defined as the variation from the “proposed design” in terms of main frontal geometrical features (e.g. joint and openings position and dimensions). This is based on the hypothesis that early-stage architectural intent is mostly driven by those features. Therefore, the index named “Variation from proposed design” of the  $i$ -th solution,  $d_{i1}$ , is defined as (obtained in a similar way to the concept of variance in statistics):

$$d_{i1} = \sqrt{\sum_j^N ((x_{ij} - x_{0j}) \cdot 100/x_{0j})^2 / N} \quad (1)$$

Where  $x_{ij}$  is the  $j$ -th frontal geometrical feature of the  $i$ -th solution generated by the optimisation engine and  $x_{0j}$  is the  $j$ -th frontal geometrical feature of the proposed design. Small values of  $d_{i1}$  represent solutions that preserve the initial architectural intent, which is intrinsically embedded in the proposed design.

The Y-axis represents the required performance, defined as the deviation of the  $i$ -th solution from a “reference point”, defined below. The index, named “Deviation from the reference point” of the  $i$ -th solution,  $d_{i2}$ , is defined as:

$$d_{i2} = \sum_k (\alpha_{ik} Y_{ik} - \alpha_{k,PF} Y_{k,RP}) \cdot A_{tot} / A_{panel} \quad (2)$$

where  $Y_{ik}$  is the value of the  $k$ -th objective function associated with the  $i$ -th solution,  $Y_{k,RP}$  is the value of the  $k$ -th objective function associated with the point, on the Pareto Front, representing the optimal choice (the “reference point”),  $A_{panel}$  is the area of the façade panel and  $A_{tot}$  is the total area covered by the façade type under investigation.  $d_{i2}$  is always defined as positive since  $\alpha_{k,PF} Y_{k,RP}$  is the smallest of all  $\alpha_{ik} Y_{ik}$ . The reference point can be found by creating a penalty function  $P$  [33], which coincides with the value of  $d_{i2}$ . Therefore,  $\alpha_k$  represent the “exchange coefficients” that describe how the penalty function varies with each the objective functions ( $\alpha_{ik} = \partial P / \partial Y_{ik}$ ). The coefficients can be either constant or variable. The ratio  $A_{tot} / A_{panel}$  represents the total number of panels. Minimising  $d_{i2}$  means selecting solutions close to the optimal one in terms of expected performance.

The radius of the  $i$ -th point on the scatterplot represents the number of knowledge-based constraints which are violated. Depending on the level of importance of each constraint, its violation can be either classified as an error (hard constraint), or as a warning (“softer” constraint). The information on whether a violated constraint is hard or soft is contained in the KB. For example, a constraint is hard if the weight of a façade panel exceeds the transportation limits, whereas the constraint can be deemed soft if a rule-of-thumb indicates a higher risk of failure (e.g. window-to-wall area above a certain limit for overheating risk, thus requiring further detailed, specialist analyses). The importance of constraints violated in each façade solution is summarised by the Weighted Constraint Score (WCS) as defined below. Furthermore, since it is desirable to have the “virtuous” solutions (i.e. solutions with few violated constraints) to be more visible in the scatterplot, an index, named Constraint Function (CF) and representing the radius of the  $i$ -th point, is defined as follows:

$$CF_i = -a \cdot WCS_i + b \quad (3)$$

$$WCS_i = A \cdot NumOfErrors + B \cdot NumOfWarnings \quad (4)$$

where  $a$  and  $b$  are coefficients to visualise the radius of the  $i$ -th point, and  $A$  and  $B$  are coefficients that assign weights to an error and a warning, respectively.  $A$  and  $B$  are characterised by a certain level of discretion. Maximising the Constraint Function means minimising the number of violated constraints (represented by the WCS) and simultaneously making the solution more visible in the diagram by increasing its radius (represented by the CF).

The goal of the optimisation is to minimise both  $d_1$  and  $d_2$ , while maximising CF. If the “proposed solution” is the optimal one, then it will have coordinates (0,0) in Figure 5. If no solution is found at coordinates (0,0), a set of non-dominated solutions (“meta-Pareto front”) will be generated that consider a trade-off between architectural intent, deviation from the reference point, and number of violated constraints represented by CF. This approach yields effective results when implemented with interactive data visualisation techniques such as HTML diagramming with the Javascript Library D3.js [34], due to the large amount of data that is generated.

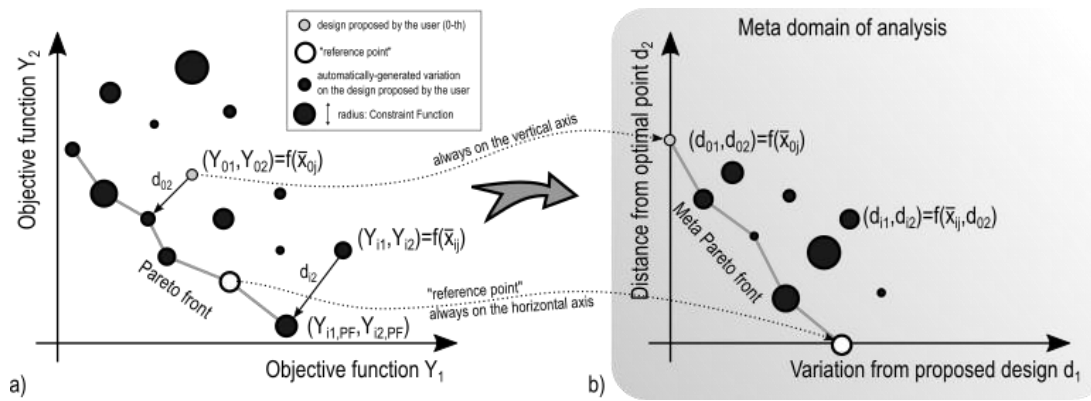


Figure 5: traditional domain of analysis in optimisation (a) and proposed “meta-domain” (b) for the optimal selection of the conceptual solution by considering the design intent.

Figure 6 shows a possible use of the proposed process in a conceptual stage. The diagram is drawn in BPMN [35], a domain-agnostic and generic notation used for modelling processes.. This diagram can be seen as a subcategory of the process maps described in Montali et al. [31]. The process is to allow the user to generate their own conceptual design, then enrich it with the knowledge-based tool, evaluate the performance and check if the design complies with the production-related constraints. Then, the user may either repeat the process normally to remove constraints that are violated or he/she chooses to run the computational optimisation to look for alternative high-performance, constraint-compliant solutions.



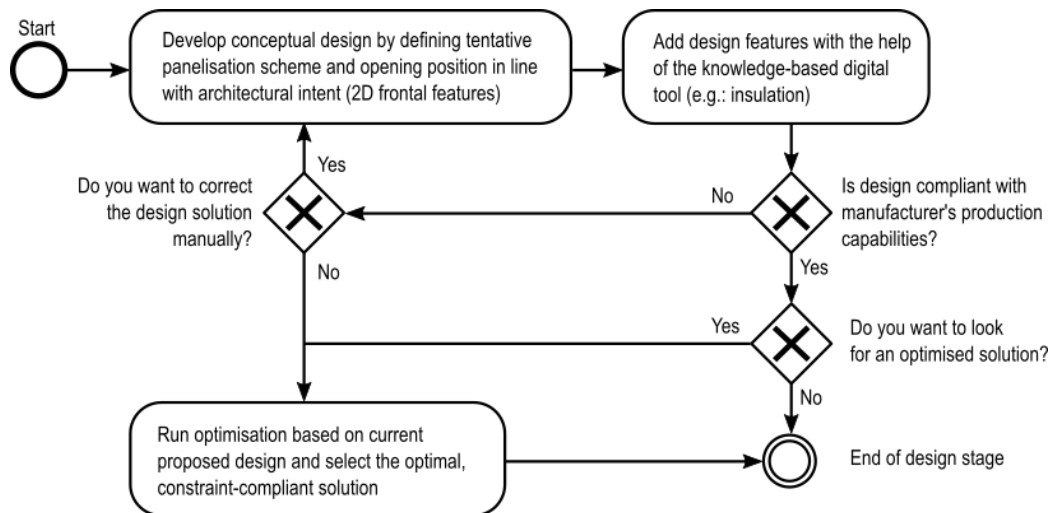


Figure 6: Proposed “enhanced” design process, in a BPMN notation, at conceptual stage incorporating optimisation by using custom-built digital tools

### 3 Application to a case study

#### 3.1 Case study

The case study consists of a recently built residential building in London. The tower is a 36-storey building clad with precast, single-leaf concrete panels. The prefabricated panels include precast concrete, insulation and window elements. The total area of the facade is 3,532m<sup>2</sup>. Once the component was installed, the dry lining, vapour control layer and plasterboard were applied onsite. Figure 7 shows the panel’s main frontal dimensions, position with respect to the primary structure and build-up. The South East façade is considered in this paper. The main motivation behind the choice of the present case study is that it is very sensitive to early-stage decisions that could affect late-stage performance; also, it is very important to define the main geometrical dimensions as early as possible in the design process, due to the prefabricated nature of the panel.

The panels were manufactured at the Explore Industrial Park, a manufacturing facility located in Steetley, Nottinghamshire (UK), part of the Laing O’Rourke Ltd group. The facility provides production lines with different degrees of automation for different types of products depending on their level of bespokeedness. The panels analysed in this paper were manufactured in the so-called “Bespoke Carousel System” (BSC), which consists of a semi-automated line. In the BSC, the panels are manufactured on a steel table which are conveyed through a series of stations where specific operations (e.g. mould lay-up, reinforcement and fitting installation, casting, panel turning for demoulding) are performed. Each station presents some manufacturing constraints and rules that affect the design of the precast panel.

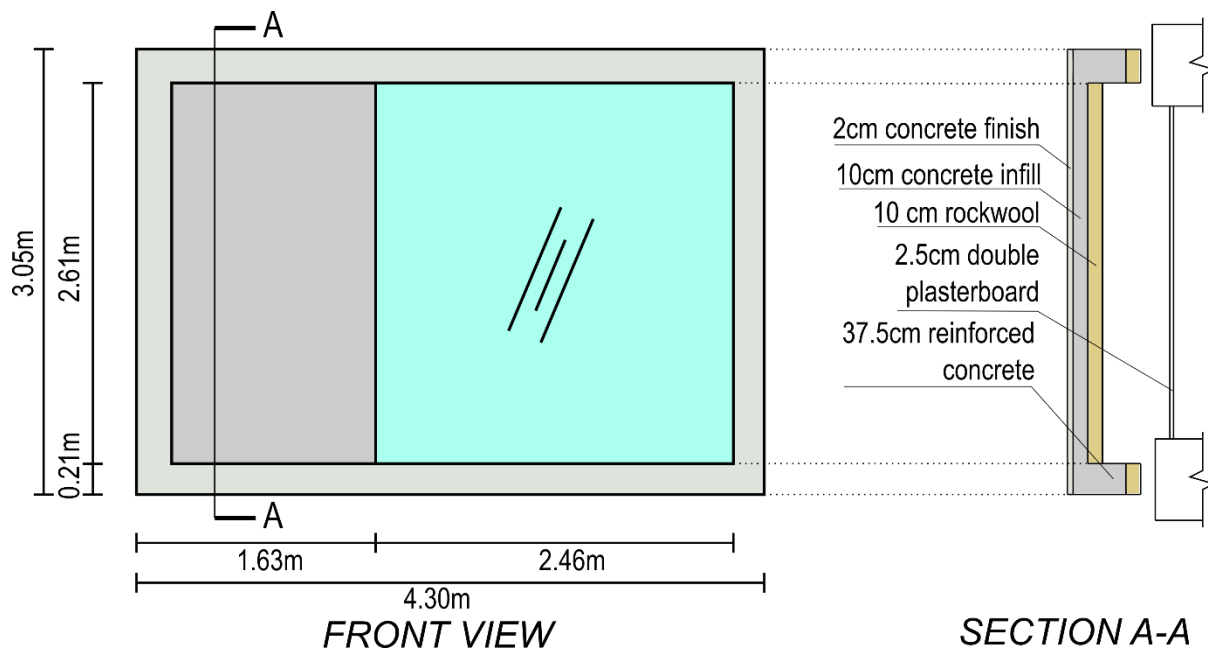


Figure 7: Main frontal dimensions (left) and build-up (right) of the investigated panel

The database used for this study comprises six types of insulation boards with different thicknesses, three types of windows (low, medium, high performance), three types of jointing materials. A knowledge-based rule governs the combination of multiple insulations (up to two) based on different criteria such as sustainability, potential installation risk from the contractor and condensation risk. Data on embodied carbon was taken from the ICE [36] V2.0 database. The database of materials used is available in the additional material that accompanies this paper.

### 3.2 Sub-process 1: how to build the knowledge base and the digital tool

The process discussed in Montali et al. [31] and developed further in in Section 2.1 (Figure 3) has been applied to the case study illustrated in Section 3.1. The following sections will illustrate the step-by-step process followed to build the final digital tool.

#### 3.2.1 Step 1: knowledge collection

The first step consisted in collecting the knowledge from relevant people within the company. Relevant people included, for instance, experts in the manufacturing division of the company giving advice on the constructability issues arising at late-stages, or people working at earlier stages on the thermal design of the panel (either directly or by supervising external consultants). All useful knowledge was then stored and used later to build the Product Model. A series of semi-structured interviews were initially conducted. To facilitate the process of knowledge collection, the interviewees were shown the latest version of the developed tool and asked to provide comments. Once the feedback about the tool was collected, the discussion moved towards adding more design and manufacturing rules/constraints to the model.

#### 3.2.2 Step 2: Knowledge base

##### Sub-step 2a

Sub-step 2a investigates the taxonomy of the product by considering the fundamental components that constitute the panel. The taxonomy is characterised by a relationship between the overall product and its constituents (in accordance with Klein's "product levels" [8]) of the type "contains". The

taxonomy for the precast, single leaf panel is shown in Figure 8, in which each element is associated with a corresponding “Entity-Structure” ICARE form that stores information about their upper- and lower- level constituents. Grey boxes represent the “leaves” of the diagram, which were then assigned a function in step b). An “Entity-Function” form was created to store a description of the function.

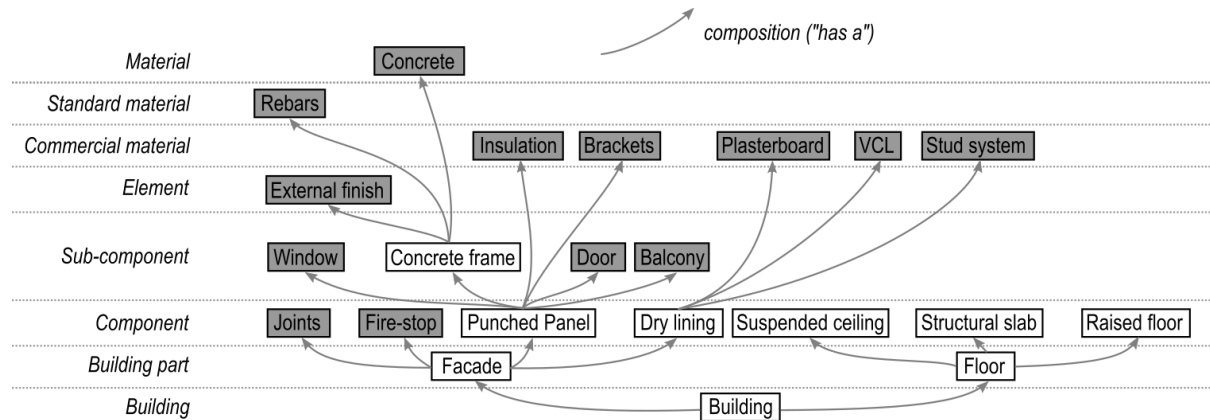


Figure 8: Taxonomy of the Product Model of precast concrete single-skin panel, based on the classification scheme proposed (“product levels”) by Klein [8]. Grey boxes represent the “leaves” of the tree.

Each component was then stored in a corresponding MOKA “Entity-structure” form. The “parent entity” or “child entity” fields of the form were filled with hyperlinks to the corresponding references to the “Entity-structure” forms representing the “whole” and the “part”, respectively<sup>2</sup>.

#### Sub-step 2b

The second part of step 2 consists of linking the product’s functions with the physical components defined in the previous sub-step. This is represented diagrammatically in the directional force-directed layout shown in Figure 9. The meaning of the directed arrow depends on the start and end elements: if an arrow points to an “Entity-structure” element (dark green circle) from an “Entity-function” element, this signifies that the link will be of the type “function associated with the physical element”. Conversely, two “Entity-structure” elements connected to another share a part-whole relationship (“has a”), as per sub-step 2a.

<sup>2</sup> Although “parent entity” and “child entity” might not be appropriate terminologies to represent the part-whole relationship, this notation has been maintained for consistency with the original MOKA forms. Future work will seek to modify such forms with façade-specific fields and fields names.



Knowledge about constraints is included into forms and it is usually applied to rules. For example, the maximum weight for lifting operation in the factory is 250kN (operated by a tandem crane) or 125kN (if operated by a single-gantry crane). This value is stored in a specific form and linked to a Rule form determining the weight of the panel.

The final product is a network of interrelated concepts, creating semantic links between features for defining product architecture, such as physical components and their functions, and design and manufacturing criteria under the form of rules and constraints. Given the large number of links between knowledge units, the final knowledge base was represented by a so-called hierarchical edge bundling, to reduce the “visual clutter when dealing with large numbers of adjacency edges” [37]. Figure 10 shows the diagram generated through the Javascript library D3.js [34].

The resulting KB works as follows. From the hierarchical edge bundling, the user can hover on specific elements such as rules, constraints, description of a physical component or its functions. The diagram is interactive in that it highlights in green all the links and interrelated elements to that specific element. If the user selects a specific element, a hyperlink redirects to a webpage containing the MOKA form describing the element in question. The form contains further links to the sources of knowledge. In the example shown in Figure 10, the user hovers on the rule “RU2114\_BracketSelection”. By clicking on the hyperlink, a webpage is opened containing the logic behind the selection of the appropriate support bracket for the precast panel. The form also contains a field (“Information origin”) with a hyperlink to a specific page of a PDF document containing the original source of knowledge. In this way, it is possible to achieve different levels of granularity of the relevant information/knowledge, from the highest level possible (the hierarchical edge bundle), to the most detailed description (the original PDF document).

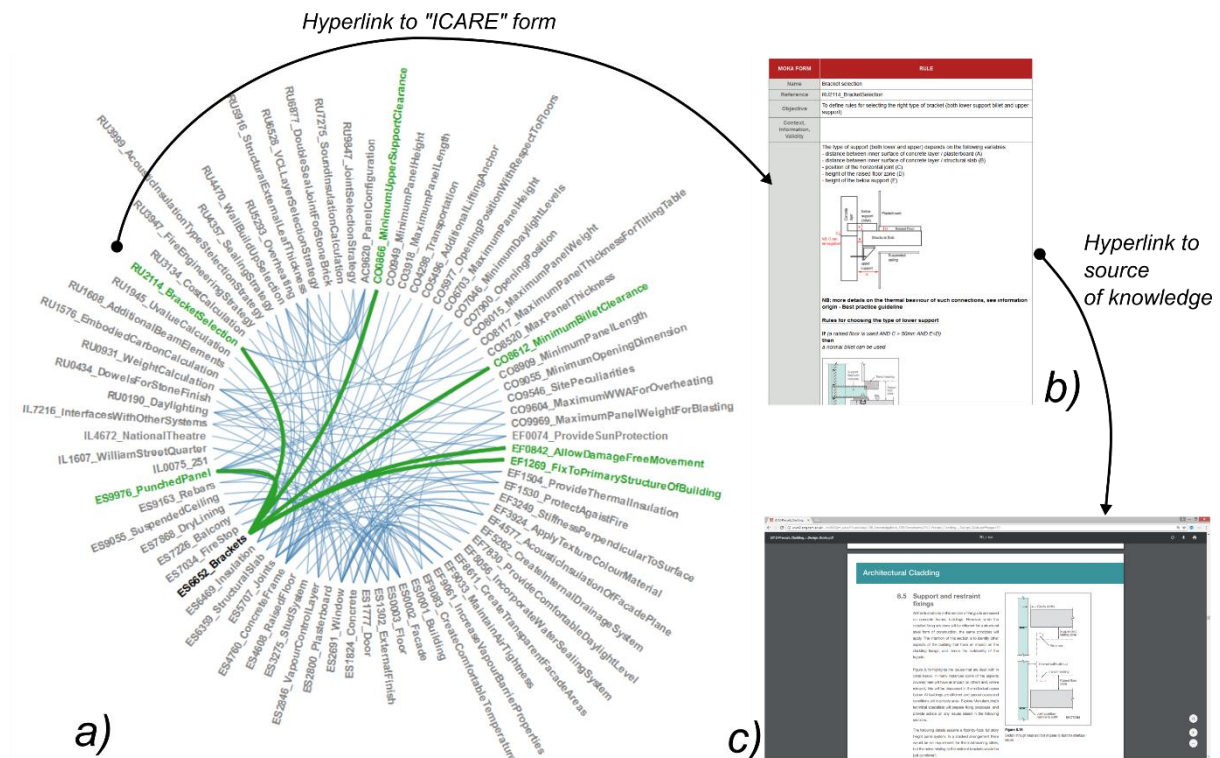


Figure 10: Knowledge base in the form of Hierarchical Edge Bundling [34,37] and links to more detailed descriptions of the underlying knowledge related to the selection of the supporting brackets for precast concrete single leaf panel: a) overarching

view of the links with other elements of knowledge, b) MOKA “Rule” form containing the logic and c) original source of knowledge.

### 3.2.3 Step 3: UML class diagramming

The definition of the fundamental components of knowledge and their storage into appropriate forms is followed by a UML class diagram to represent the product architecture for the subsequent implementation. Figure 11 shows the generated diagram, in which each class represents a physical component. Functions (e.g. thermal) and properties (e.g. weight) are assigned via interfaces that are implemented by the classes. In some cases, interfaces were not assigned to certain elements since they have a negligible effect on the performance of the panel (e.g. vapour control layer on weight).

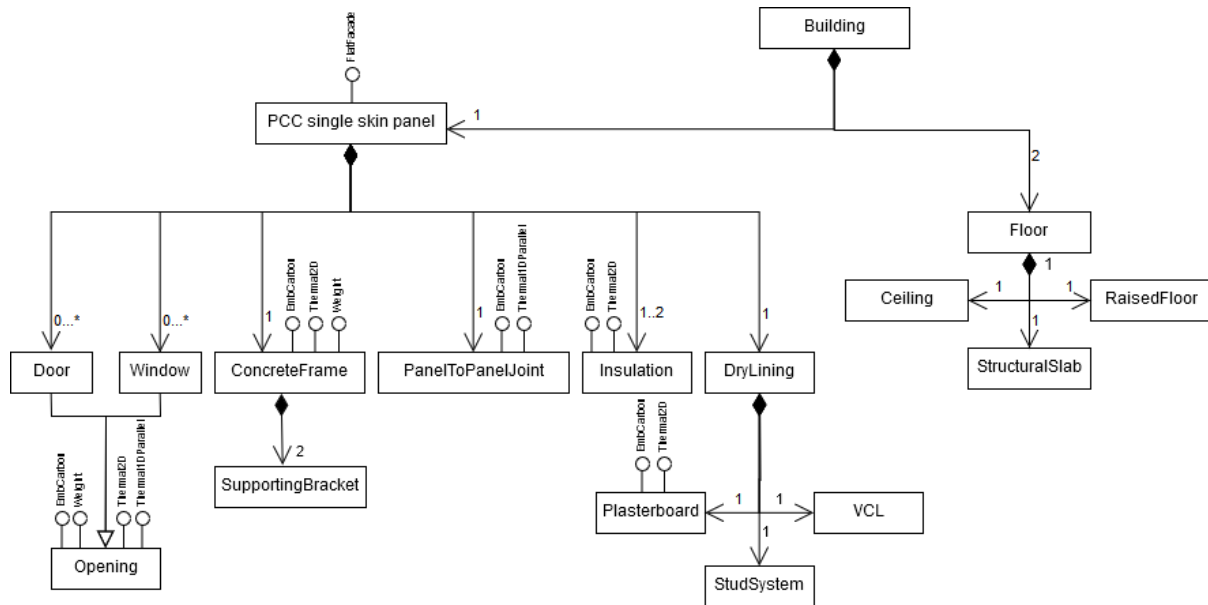


Figure 11: UML diagram representation of the product architecture

For example, the “PanelToPanelJoint” class function implements the “IThermal1DParallel” interface since joints are one-dimensional elements, parallel to the surface of the façade, that dissipate energy through the linear thermal transmittance along the length of the joint. Thus, the interface requires all elements that implement the class to include the two properties “psi” and “length”.

```
public interface IThermal1DParallel
{
    double psi { get; set; }
    double length { get; set; }
}
```

### 3.2.4 Step 4: digital tool implementation

The last step consists of the implementation of the PM into a usable digital tool. The tool shown here constitutes an evolution from an earlier version [38], after several iterations of the process shown in Figure 3. The chosen platform is Rhinoceros 5 by McNeel Associates [39] and the tool was under the form of a series of Grasshopper’s custom components written in C# representing the Product Model (Figure 12). Once the user has drawn the surface representing the overall façade, a specific Grasshopper definition is associated to the surface. Figure 12a shows the window to configure the panel in terms of build-up, the type of jointing solutions, the external finish type, as well as other properties such as the thickness of the concrete layer (which can be automatically determined based on the rule described in sub-step 2c) or the thickness of the air layer. All configurations are selected



from a pre-built set of solutions, which embed knowledge about the preferred design and manufacturing practices from the manufacturer. Figure 12b shows a series of performance indices are automatically calculated based on the selected configuration, such as U-value, daylight factor, embodied carbon, panel weight and total panel thickness. Figure 12c contains the KB shown in section 2.1, which is updated automatically as the user configures the PM. If a “hard constraint” is violated, then the corresponding element will turn red; if the broken constraint is “soft”, then the text will turn orange. In this way, the user is informed about the consequences of their design choices. Figure 12d shows that is also possible to determine an early-stage estimate of the expected operational energy or carbon by running a dynamic, single zone energy simulation at run-time via a link to Energy Plus [40], based on the solution that is currently configured by the user.

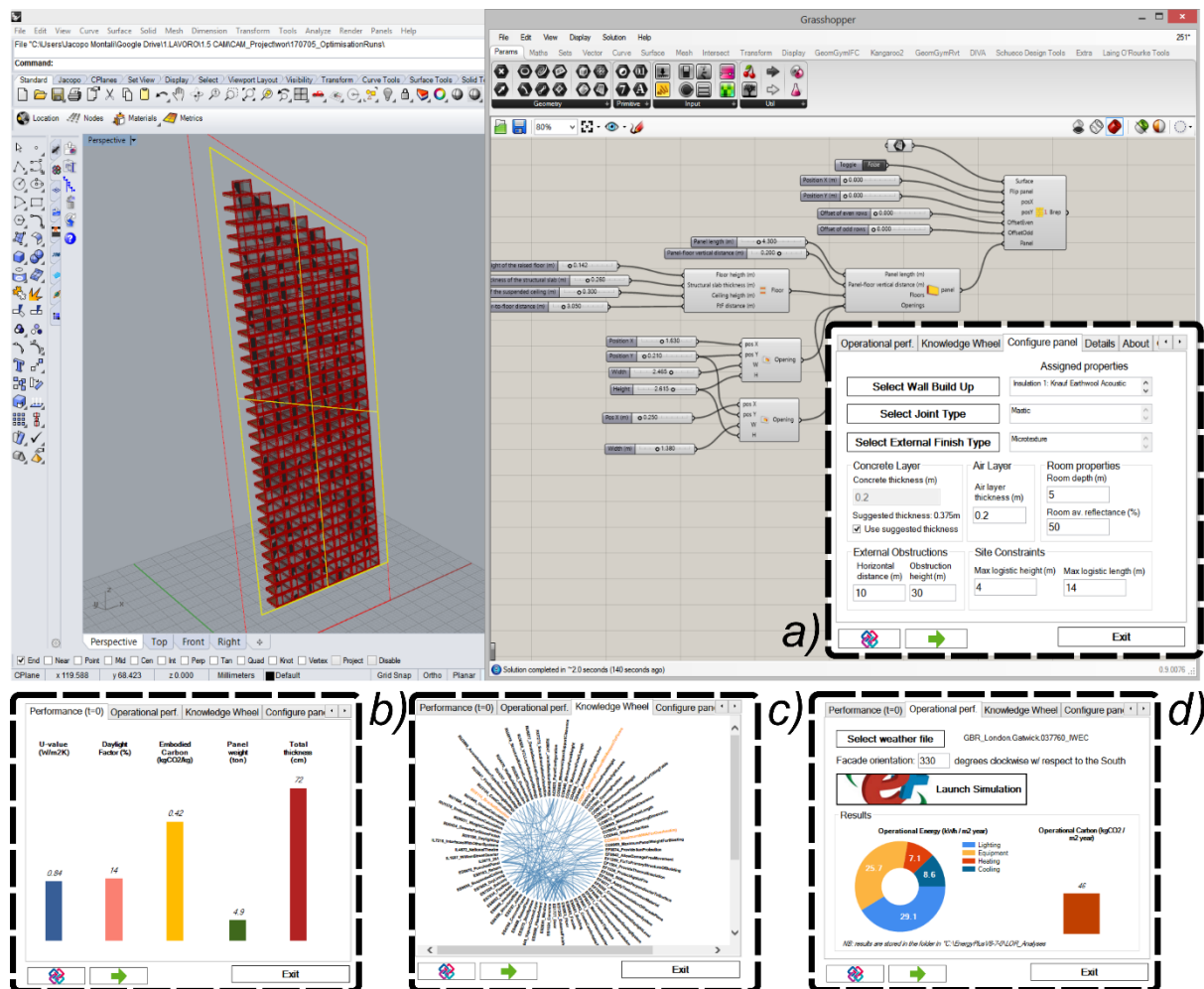


Figure 12: Digital tool's GUI for panel build-up configuration (a), performance analysis (b), compliance to constraints (c), and operational performance via Energy Plus (d)

### 3.3 Sub-process 2: optimisation

#### 3.3.1 The optimisation algorithm

The knowledge base and the digital tools serve as a configuration tools to understand trade-offs between design criteria. The approach that follows builds upon the first sub-process and seeks for an optimised solution that takes into account for the optimal trade-off between performance, number

of violated Design and Manufacturing constraints and adherence to the initially-conceived architectural intent.

The optimisation process described in Section 2.2 was applied to identify an optimised solution. The objective functions chosen in this instance are operational carbon ( $Y_{i1}$ , measured in kgCO<sub>2</sub>/y·m<sup>2</sup> of floor area) and embodied carbon ( $Y_{i2}$ , measures in kgCO<sub>2</sub>/kg of panel weight). The deviation from the reference point of the  $i$ -th solution  $d_{i2}$  is therefore equal to:

$$d_{i2} = [\alpha_{i1}(Y_{i1} - Y_{i1,RP}) + \alpha_{i2}(Y_{i2} - Y_{i2,RP})] \cdot A_{tot}/A_{panel} \quad (7)$$

The penalty function  $d_{i2}$  presents the following two coefficients  $\alpha_{i1}$  and  $\alpha_{i2}$ , which will be variable with the  $i$ -th solution:

$$\alpha_{i1} = T \cdot D \cdot L \quad (8)$$

$$\alpha_{i2} = W \quad (9)$$

where, for the specific case,  $T$  is the service life of the facade (equal to 20 years),  $D$  is the room depth (equal to 5 m),  $L$  is the panel length identifying the room width, and  $W$  is the total weight of the panel. Note that  $L$ ,  $W$ ,  $A_{panel}$  and  $A_{tot}$  depend on the  $i$ -th solution: the digital tool will automatically calculate the value of the coefficients at runtime.

The operational energy was determined computationally by means of a building performance dynamic simulation in Energy Plus (v8.7). This involved creating a single-zone model with adiabatic surfaces except for the facade under investigation. In this model, the width of the zone corresponds to the width of the panel, which does not necessarily correspond to the room width. For this reason, the analysis should be seen as conducted over the area of influence of the façade, rather than a specific room. A “Building Area Method” as per ASHRAE 90.1 [41] was therefore followed, in which internal gains are given for generic end uses, rather than for specific space types (e.g.: office vs open office or single office). This approach is particularly suitable for early-stage conceptual stages, where the internal distribution of spaces is poorly defined. The template of the .IDF file used for the analysis is available in the additional data that accompanies this paper.

A custom-built, random-generating of trials algorithms was used to apply at run-time the knowledge-based network of rules and constraints and to incorporate them into the analysis. The following pseudocode describes the internal logic of the algorithm:

```

for (int i = 0; i < numOfCycles; i++)
{
    // Generate randomic variation from the proposed design, based on a maximum variation
    sibling = GenerateSibling(...,maxVariation);

    // Check if openings are not placed correctly and update number of invalid analyses
    if (openingPositionIsCorrect(sibling) == false) {
        numOfNonValidAnalyses++;
        continue; }

    // Evaluate solution outputs
    output = EvaluateSolution(sibling);

    // Store input and output values
    UpdateOutput(sibling, output);
}

```



The algorithm iterates over a specified number of cycles (numOfCycles), thus allowing the user to control the calculation time. The algorithm generates a variation of both the frontal dimensions of the panel and the continuous variables governing the thicknesses of the internal build-up (e.g. thickness of the air layer) based on a certain user-defined maxVariation expressed as a percentage. Continuous variables  $x_i$  are drawn from a normal Gaussian distribution with zero mean and variance  $\sigma$ :

$$x_i \sim N(x_i|0, \sigma) = x_i + \sigma \cdot N(0,1) \quad (10)$$

where  $\sigma$  is equal to  $0.5 \cdot \text{maxVariation}$ , so that there is a  $\sim 95\%$  confidence interval that each sampled feature falls within the maxVariation, while allowing a  $\sim 5\%$  of outliers. The sampling was implemented via Box-Muller transformation. Discrete variables  $A_j$  are instead sampled from a uniform distribution:

$$A_j \sim U(0, K) \quad (11)$$

Where  $K$  is the total number of discrete variables for the  $j$ -th discrete feature.

*Table 1: Continuous and discrete variables governing the design of the panel. The variation of these variables has been drawn from a Gaussian and a uniform distribution, respectively.*

Continuous variables $x_i$	Discrete variables $A_j$
Panel height and width	Type of wall build-up
Relative position of panel w.r.t. primary structure	Type(s) and thickness(es) of insulation
Air layer thickness	Type(s) of window
Window(s) position within the panel	
Window(s) height and width	
Concrete infill(s) position within the panel	
Concrete infill(s) height and width	

### 3.3.2 Results from the optimisation

Analyses were run on a Dell Inspiron with 8GB RAM and processor Intel Core i7-3630 QM, 2.40GHz. The same optimisation was run three times with three different values for the parameter numOfCycles (150, 1500, 15000), whereas the parameter maxVariation was set to 10%. Calculation times were 8h, 2h and 20mins, respectively. The number of discarded analyses due to unfeasible geometries (e.g. window outline overlapping panel outline) was equal to 46, 473 and 4722, respectively.

The results were also compared with what obtained from a Genetic Algorithm (GA) approach, which represents the benchmark for the analyses that were run. The prototype whole-life value optimization tool for façade design model [21] was adapted to take into account the variables and objectives in this study. While the database of materials was incorporated in the GA, design knowledge from the knowledge base was not included due to confidentiality reasons. For the implementation of the genetic algorithm, a convergence test was carried out for different population sizes and numbers of generations. A population size of 1000 and number of generation of 50 was selected to ensure that a close approximation of the real Pareto Front can be obtained. The crossover probability was set to 70% in the algorithm. Analyses were run on a Windows with 8GB RAM and processor Intel Core i7-4650 U, 1.70GHz. The total simulation time is 32hrs for the GA optimisation.

Figure 13 shows the results from the optimisation. Results can also be accessed [here<sup>3</sup>](#) for an interactive view. The interactive diagram also shows the governing parameters and performance / violated constraints of every solution.

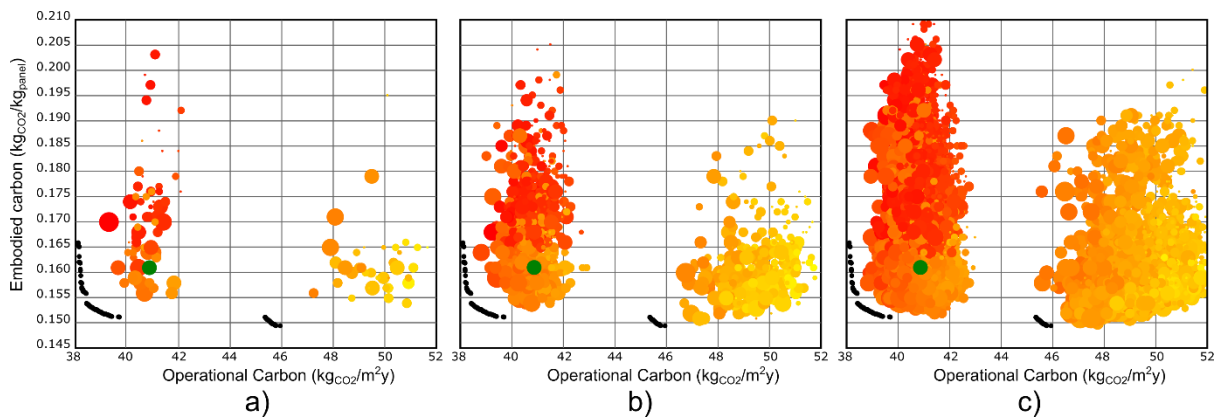


Figure 13: Results from the optimisation of the case study. Analyses for “numOfCycles” equal to 150 (a), 1500 (b) and 15000 (c), respectively. “maxVariation” was set to 10%. The colour scale from light yellow to red refers to increasing levels of overall U-value. Black points correspond to the values obtained from the GA optimisation. The green point is the original “proposed design”.

Results were then elaborated and transferred to the “meta-domain” of analysis, in which the indices  $d_1$ ,  $d_2$  and CF are shown (Figure 14). The vertical axis represents the total carbon difference between the  $i$ -th solution and the reference point ( $d_2 = 0$ ). Solutions close to the (0,0) point are both environmentally optimised and follow the initial design intent. The diagram therefore illustrates how modifying the solution towards optimality requires a corresponding modification to the original proposed design ( $d_1 = 0$ ). Figure 14 shows the generated diagrams for the three analyses. A large radius represents few broken constraints in terms of performance and manufacturability. An additional information is here added by the colour, representing the total panel’s thickness. Large radii mean low number of violated constraints.

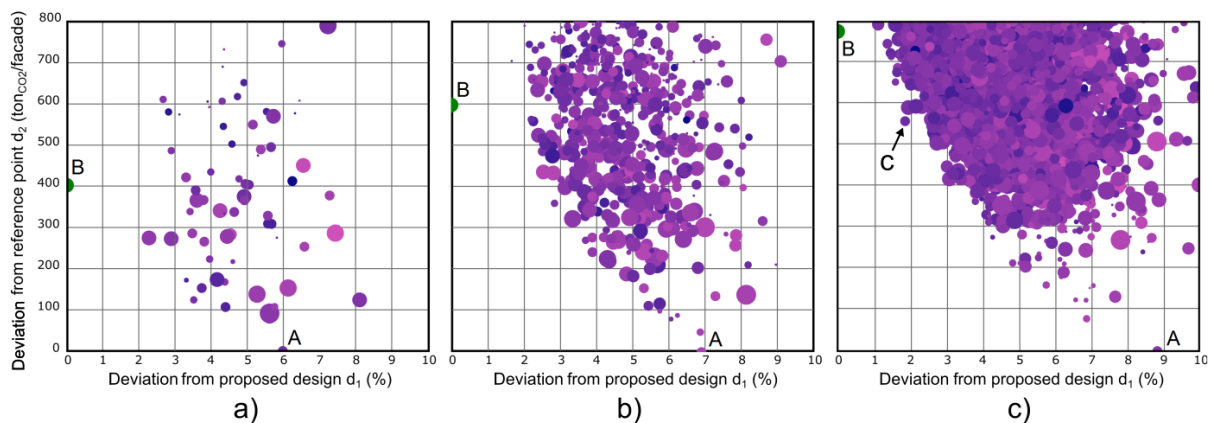


Figure 14: “Meta-domain” of analysis for the case study, corresponding to the analyses showed in Figure 13. The colour scale from light to dark purple refers to increasing levels of panel’s total thickness. Points A and B represent the optimal solution for the two objective functions and the original proposed design, respectively. Point C represents a chosen solution which performs better than the original design.

<sup>3</sup> <https://bit.ly/2HUEb0l>

## 4 Discussion

Results shown in Figure 13 indicate that the initially-proposed configuration (green circle) is not the optimal one. This is evident even if few analyses are run (150 in Figure 13a). Moreover, solutions associated with very low U-values do not constitute optimal trade-offs between embodied and operational energy: given the relatively large window-to-wall area of this study (circa 40%), the optimal solutions instead correspond to an intermediate level of specification of the window (orange). This is caused by the increased need for cooling energy in the London climate. The incidence of the window type also determined two separate groups of solutions, one corresponding to the low performance window, and one associated with the remaining two (mid- and high-performance) window types. The radii of the solutions (i.e. design and manufacturing constraints) do not follow a specific trend, but the interactive visualisation technique allows the user to browse through each solution individually. The constraints that were affected by the modifications in the range of the proposed design (maxVariation = 10%) regarded the choice of the type of structurally-supporting bracket at the bottom of the joints and the position of the opening being too close to the edge of the panel.

The average distance between the generated Pareto front and the one obtained from the GA approach tended to reduce with the “numOfCycles” parameter. In general, optimal solutions from the GA algorithm showed geometrical frontal features (panel width and height) tending towards their limits imposed for the GA optimisation.

The proposed meta-domain (Figure 14) includes the architectural intent into the decision-making process via the “Variation from proposed design” of the  $i$ -th solution,  $d_{i1}$ . The diagrams are characterised by two extreme points: the proposed solution (point “B”), which lies on the Y-axis ( $d_{i1} = 0$  and  $d_{i2} \neq 0$ ), and the solution (point “A”), on X-axis, that has the lowest value of  $d_{i2}$  ( $d_{i1} \neq 0$  and  $d_{i2} = 0$  in this case). The latter is the solution, on the Pareto front, that is geometrically more similar to the proposed design. No point with both  $d_{i1} = 0$  and  $d_{i2} = 0$  was determined, which corresponds to the case when the proposed solution lies exactly on the Pareto front. Table 2 summarises the values of  $d_1$  and  $d_2$  for these two extreme points for the three analyses. The remaining non-dominated solutions in the meta-domain represent optimal trade-offs between the whole carbon savings and the architectural expression. Non-dominated solutions thus allow for more geometrical diversity in favour of a lower environmental impact. In general, the larger the number of analyses, the larger the deviation from the reference point, and therefore the less environmentally friendly the proposed solution will be. There is therefore an additional trade-off between the complexity/time to run the optimisation and the potentially-achievable carbon savings.

The proposed approach presents two distinct aspects. The first aspect is the focus on the implementation of design knowledge and its representation in interactive diagrams. This allows the user to browse through a variety of different solutions and understand their performance and compliance to a broad spectrum of design and manufacturing constraints. The second aspect is the ability to explore the “deviations” of optimised solutions from the originally-conceived solution. The deviations take into account for both performance-based criteria and the architect’s design intent.

*Table 2: Values of  $d_1$ ,  $d_2$  and CF for the two extreme points A ( $d_{i1} \neq 0$ ,  $d_{i2} = 0$ ) and B ( $d_{i1} = 0$ ,  $d_{i2} \neq 0$ ) of the meta-Pareto front for the three analyses.*

Number of cycles
------------------

	150		1500		15000	
	Point A	Point B	Point A	Point B	Point A	Point B
Deviation from proposed design $d_{i1}$	5.98%	0	6.90%	0	8.84%	0
Deviation from reference point $d_{i2}$	0	402.51 $t_{CO2}$	0	597.67 $t_{CO2}$	0	776.67 $t_{CO2}$
Weighted Constraint Score	2.5	1.5	2.5	1.5	2.5	1.5

A typical usage scenario for the above diagrams would include the selection of the best solutions on the meta-front starting from solutions with the lowest distance from the originally-intended design. Figure 15b shows an example of a design solution that improves the performance of the proposed design while keeping the aesthetical variation from the originally-intended design (Figure 15a) to the minimum ( $d_1 = 1.86\%$ ). The solution in Figure 15b was chosen from the analysis with numOfCycles=15000 (point C in Figure 14c). The different aesthetical appearance of the solution, combined with the variation in the material properties, led to a reduction of 218  $t_{CO2}$  for the whole façade from the initially-intended design. This is mostly due to the reduction in insulation material and concrete thickness, as well as to the reduced Window-To-Wall area. However, this solution presents a Weighted Constraint Score equal to 2.5, 1 point higher than the original design. This is due to the presence of a design error regarding the absence of a minimum clearance of 20cm on the supporting structural slab (Figure 15c). Therefore, designers either need to find solutions to support the panel with less clearance (e.g. by developing a more engineered solution) or by moving down the meta-front to look for solutions with lower Weighted Constraint Scores (and lower  $d_2$ ), even if the aesthetical deviation from the proposed design  $d_1$  increases (Figure 14d).

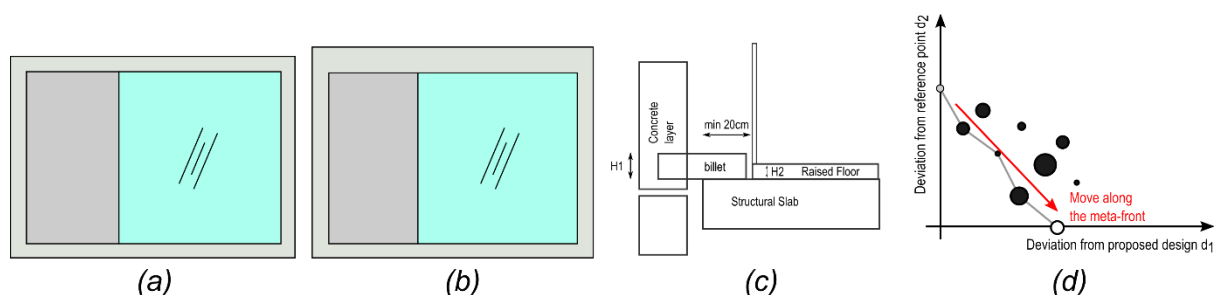


Figure 15: Comparison between (a) the original design (point B in Figure 14c) and (b) the chosen design solution that improves the performance of the original design (point C in Figure 14c). Despite performing better, this solution presents an error in the position of the structural billet, which requires a minimum 20cm clearance on the structural slab (c). A possible option is to move further down-left along the meta-front (d).

## 5 Conclusion

The present paper shows an approach that makes downstream knowledge (i.e. manufacturing) readily available for use in upstream processes (i.e. early stage design) to achieve optimised design solutions. The current state of optimisation in façade design focuses on the use of very specific (namely, GA) techniques applied to few domains of interest (e.g. thermal behaviour). This approach captures only partially the interrelationships underlying the design of the product, as the majority of the effort is

dedicated to the optimisation algorithm at the expense of the knowledge capture stage. For this reason, more emphasis should be put in the analysis of the product architecture, and in the collection and formalisation of the available design knowledge, even at the expense of obtaining more approximate values of the objective functions. The present paper introduces a two-step process for determining the optimal solution in terms of multiple criteria when configuring a specific facade product at early design stages. The first step requires the identification of the product architecture and sets the ground to integrate design and manufacturing knowledge into a single, interactive knowledge base for product configuration. It is a process at the boundaries of knowledge management, data visualisation, digital technologies, and engineering. The construction of the knowledge base has allowed a comprehensive overview of the underlying knowledge behind the design and manufacture of a real-world facade product manufactured by a specific supplier. The implementation of rules and constraints into an existing platform (Rhinceros and Grasshopper) has allowed the automatic use of such criteria for design purposes. Although the approach has been applied to a specific case-study of a precast panel, its generality makes it applicable to other system types. As an example, unitised façades are highly prefabricated systems that require early capture of the fundamental criteria governing thermal and structural behaviour, manufacturing limits and logistics.

The second step involves a decision-making procedure for choosing between a set of non-dominated solutions characterised by specific performance indices. The process creates a “meta-domain” of analysis to find trade-offs between performance and architectural intent, while allowing for maximum compliance to manufacturing, logistic and design constraints. Those constraints are not treated as “hard” and as such, innovation is still possible by exploring apparently non-compliant solutions. Limitations on the choice of points on the Pareto front are therefore addressed and partially reduced: the meta-front is more selective, more readable and richer than a traditional Pareto front, that does not give insights on the architectural intent and manufacturability/buildability criteria.

Further work is required to investigate the increased quality, reduced design costs and time by using such tool. Future work will thus include testing the tool by running workshops with sector experts to quantify the benefits arising from such novel approach.

## Acknowledgements

The authors would like to thank the Engineering and Physical Science Research Council (EPSRC) and Laing O’Rourke Plc for supporting the present research programme.

## References

- [1] HM UK Government, Industrial Strategy: government and industry in partnership - Construction 2025, 2013. [https://www.gov.uk/government/uploads/system/uploads/attachment\\_data/file/210099/bis-13-955-construction-2025-industrial-strategy.pdf](https://www.gov.uk/government/uploads/system/uploads/attachment_data/file/210099/bis-13-955-construction-2025-industrial-strategy.pdf).
- [2] European Parliament, Directive 2012/27/EU of the European Parliament and of the Council of 25 October 2012 on energy efficiency, amending Directives 2009/125/EC and 2010/30/EU and

- 623 repealing Directives 2004/8/EC and 2006/32/EC Text with EEA relevance, 2012. [http://eur-](http://eur-lex.europa.eu/legal-content/EN/TXT/HTML/?uri=CELEX:32012L0027&from=EN)  
624 [lex.europa.eu/legal-content/EN/TXT/HTML/?uri=CELEX:32012L0027&from=EN](http://eur-lex.europa.eu/legal-content/EN/TXT/HTML/?uri=CELEX:32012L0027&from=EN).
- 625 [3] M. Kassem, D. Mitchell, Bridging the gap between selection decisions of facade systems at the  
626 early design phase: Issues, challenges and solutions, *Journal of Facade Design and Engineering*. 3  
627 (2015) 165–183. doi:10.3233/FDE-150037.
- 628 [4] The Economist, The construction industry's productivity problem (2017).  
629 <https://www.economist.com/leaders/2017/08/17/the-construction-industrys-productivity-problem>.  
630 (accessed August 17, 2017)
- 631 [5] Construction Industry Council, Offsite Housing Review, (2013) 1–43.  
632 <http://cic.org.uk/download.php?f=offsite-housing-review-feb-2013-for-web.pdf>.
- 633 [6] McKinsey & Company, The construction productivity imperative, (2015).  
634 [www.mckinsey.com/industries/capital-projects-and-infrastructure/our-insights/the-construction-](http://www.mckinsey.com/industries/capital-projects-and-infrastructure/our-insights/the-construction-productivity-imperative)  
635 [productivity-imperative](http://www.mckinsey.com/industries/capital-projects-and-infrastructure/our-insights/the-construction-productivity-imperative). (accessed September 10, 2017)
- 636 [7] Knowledge Transfer Network, High Value Manufacturing - Modelling and Simulation Best  
637 Practice (SimBest) - Best Practice Final Report, (2016).  
638 [https://www.google.com/url?sa=t&rct=j&q=&esrc=s&source=web&cd=3&ved=2ahUKEwiX-](https://www.google.com/url?sa=t&rct=j&q=&esrc=s&source=web&cd=3&ved=2ahUKEwiX-Zym9M3cAhVJqaQKHrtcBJsQFjACegQICBAC&url=https%3A%2F%2Fepsr.ukri.org%2Ffiles%2Ffundin)  
639 [Zym9M3cAhVJqaQKHrtcBJsQFjACegQICBAC&url=https%3A%2F%2Fepsr.ukri.org%2Ffiles%2Ffundin](https://www.google.com/url?sa=t&rct=j&q=&esrc=s&source=web&cd=3&ved=2ahUKEwiX-Zym9M3cAhVJqaQKHrtcBJsQFjACegQICBAC&url=https%3A%2F%2Fepsr.ukri.org%2Ffiles%2Ffundin)  
640 [g%2Fcalls%2F2015%2Fsimulation-and-modelling-best-practice-workshop-](https://www.google.com/url?sa=t&rct=j&q=&esrc=s&source=web&cd=3&ved=2ahUKEwiX-Zym9M3cAhVJqaQKHrtcBJsQFjACegQICBAC&url=https%3A%2F%2Fepsr.ukri.org%2Ffiles%2Ffundin)  
641 [outputs%2F&usg=AOvVaw0UIal5bAUygUFsZIGOFFIO](https://www.google.com/url?sa=t&rct=j&q=&esrc=s&source=web&cd=3&ved=2ahUKEwiX-Zym9M3cAhVJqaQKHrtcBJsQFjACegQICBAC&url=https%3A%2F%2Fepsr.ukri.org%2Ffiles%2Ffundin).
- 642 [8] T. Klein, *Integral Façade Construction - Towards a New Product Architecture for Curtain Walls*,  
643 2013. isbn: 9789461861610.
- 644 [9] E. Voss, Q. Jin, M. Overend, A BPMN-Based Process Map for the Design and Construction of  
645 Façades, *Journal of Facade Design and Engineering*. 1 (2013) 17–29. doi:10.3233/FDE-130006.
- 646 [10] G. Boothroyd, P. Dewhurst, W. Knight, *Product Design for Manufacture and Assembly*, 3rd ed,  
647 CRC Press, 2010. isbn: 978-1-4200-8928-8, 1420089285.
- 648 [11] J. Heyman, *The Stone Skeleton: Structural Engineering of Masonry Architecture*, Cambridge  
649 University Press, 1997. isbn: 978-0521629638.
- 650 [12] J. Montali, M. Overend, P.M. Pelken, M. Sauchelli, Knowledge-Based Engineering in the design  
651 for manufacture of prefabricated façades: current gaps and future trends, *Architectural Engineering*  
652 *and Design Management*. 0 (2017) 1–17. doi:10.1080/17452007.2017.1364216.
- 653 [13] Herzog, Thomas, *Facade Construction Manual*, 1st ed, Birkhauser-Publishers for Architecture,  
654 Basel ; Boston ; Berlin, 2004. isbn: 3764371099.
- 655 [14] K. Ulrich, The Role of Product Architecture in the Manufacturing Firm, *Research Policy*. 24  
656 (1995) 419–440. doi:10.1016/0048-7333(94)00775-3.
- 657 [15] V. Karhu, Product Model Based Design of Precast Facades, *Electronic Journal of Information*  
658 *Technology in Construction*. 2 (1997). <http://www.itcon.org/1997/1>.

- 659 [16] H.M. Said, T. Chalasani, S. Logan, Exterior prefabricated panelized walls platform optimization,  
660 Automation in Construction. 76 (2017) 1–13. doi:10.1016/j.autcon.2017.01.002.
- 661 [17] A. Fuchs, S. Peters, O. Hans, J. Möhring, Schüco Parametric System - Uniqueness in Series, in:  
662 Advanced Building Skins, Graatz, 2015. isbn: 978-3-98120538-1.
- 663 [18] T. Henriksen, S. Lo, U. Knaack, The impact of a new mould system as part of a novel  
664 manufacturing process for complex geometry thin-walled GFRC, Architectural Engineering and Design  
665 Management. 12 (2016) 231–249. doi:10.1080/17452007.2016.1159540.
- 666 [19] M. Belsky, R. Sacks, I. Brilakis, Semantic Enrichment for Building Information Modeling,  
667 Computer-Aided Civil and Infrastructure Engineering. 31 (2015) 261–274. doi:10.1111/mice.12128.
- 668 [20] C. Eastman, J.M. Lee, Y.S. Jeong, J.K. Lee, Automatic Rule-Based Checking of Building Designs,  
669 Automation in Construction. 18 (2009) 1011–1033. doi:10.1016/j.autcon.2009.07.002.
- 670 [21] Q. Jin, M. Overend, A prototype whole-life value optimization tool for façade design, Journal  
671 of Building Performance Simulation. 1493 (2013). doi:10.1080/19401493.2013.812145.
- 672 [22] G. Zemella, D. De March, M. Borrotti, I. Poli, Optimised design of energy efficient building  
673 facades via Evolutionary Neural Networks, Energy & Buildings. 43 (2011) 3297–3302.  
674 doi:10.1016/j.enbuild.2011.10.006.
- 675 [23] E. Znouda, N. Ghrab-morcos, A. Hadj-alouane, Optimization of Mediterranean building design  
676 using genetic algorithms, Energy and Buildings. 39 (2007) 148–153.  
677 doi:10.1016/j.enbuild.2005.11.015.
- 678 [24] F. Favoino, F. Fiorito, A. Cannavale, G. Ranzi, M. Overend, Optimal control and performance  
679 of photovoltachromic switchable glazing for building integration in temperate climates, Applied  
680 Energy. 178 (2016) 943–961. doi:10.1016/j.apenergy.2016.06.107.
- 681 [25] C. Kasinalis, R.C.G.M. Loonen, D. Cóstola, J.L.M. Hensen, Framework for assessing the  
682 performance potential of seasonally adaptable facades using multi-objective optimization, Energy &  
683 Buildings. 79 (2014) 106–113. doi:10.1016/j.enbuild.2014.04.045.
- 684 [26] F. Favoino, Q. Jin, M. Overend, Design and control optimisation of adaptive insulation systems  
685 for office buildings . Part 1 : Adaptive technologies and simulation framework, Energy. 127 (2017)  
686 301–309. doi:10.1016/j.energy.2017.03.083.
- 687 [27] Q. Jin, F. Favoino, M. Overend, Design and control optimisation of adaptive insulation systems  
688 for office buildings . Part 2 : A parametric study for a temperate climate, Energy. 127 (2017) 634–649.  
689 doi:10.1016/j.energy.2017.03.096.
- 690 [28] J. Wallner, H. Pottmann, Geometric computing for freeform architecture, Journal of  
691 Mathematics in Industry. (2011). doi:10.1186/2190-5983-1-4.
- 692 [29] M. Eigensatz, M. Deuss, A. Schiftner, M. Kilian, N.J. Mitra, H. Pottmann, M. Pauly, Case Studies  
693 in Cost-Optimized Paneling of Architectural Freeform Surfaces, in: C. Ceccato, L. Hesselgren, M. Pauly,



694 H. Pottmann, J. Wallner (Eds.), *Advances in Architectural Geometry* 2010, Springer Vienna, Vienna,  
695 2010: pp. 49–72. isbn: 978-3-7091-0309-8.

696 [30] H. Pottmann, Y. Liu, J. Wallner, A. Bobenko, W. Wang, *Geometry of Multi-layer Freeform*  
697 *Structures for Architecture*, 26 (2007). doi:10.1145/1239451.1239516.

698 [31] J. Montali, M. Overend, P.M. Pelken, M. Sauchelli, *Towards facades as Make-To-Order*  
699 *products--the role of Knowledge-Based-Engineering to support design*, *Journal of Facade Design and*  
700 *Engineering*. 5 (2017) 101–112. doi:http://dx.doi.org/10.7480/jfde.2017.2.1744.

701 [32] M. Stokes, *Managing Engineering Knowledge – MOKA: Methodology for Knowledge Based*  
702 *Engineering Applications*, American Society of Mechanical Engineers, 2001. isbn: 978-1-860-58295-0.

703 [33] M.F. Ashby, *Multiple Constraints and Conflicting Objectives*, in: *Materials Selection in*  
704 *Mechanical Design*, 4th ed., Elsevier, 2011: pp. 197–216. doi:10.1016/B978-1-85617-663-7.00008-4.

705 [34] M. Bostock, V. Ogievetsky, J. Heer, *D3: Data-Driven Documents*, in: *IEEE (Ed.), IEEE*  
706 *Transactions on Visualization & Computer Graphics*, 2011: pp. 2301–2309.  
707 doi:10.1109/TVCG.2011.185.

708 [35] BPMN, (2017). <http://www.bpmn.org/>. (accessed June 22, 2017)

709 [36] G.P. Hammond, C.I. Jones, *Embodied energy and carbon in construction materials*,  
710 *Proceedings of the Institution of Civil Engineers - Energy*. (2008). doi:10.1680/ener.2008.161.2.87.

711 [37] D. Holten, *Hierarchical Edge Bundles: Visualization of Adjacency Relations in Hierarchical Data*,  
712 *IEEE Transactions on Visualization and Computer Graphics*. 12 (2006) 741–748.  
713 doi:10.1109/TVCG.2006.147.

714 [38] J. Montali, M. Overend, P.M. Pelken, M. Sauchelli, *Knowledge-Based Engineering Applications*  
715 *for Supporting the Design of Precast Concrete Façade Panels*, in: *ICED17: International Conference of*  
716 *Engineering Design*, Vancouver, 2017. issn: 22204342.

717 [39] Robert McNeel & Associates, *Rhinoceros webpage*, (2017). <https://www.rhino3d.com/>.  
718 (accessed October 18, 2017)

719 [40] D.B. Crawley, C.O. Pedersen, L.K. Lawrie, F.C. Winkelmann, *EnergyPlus: Energy Simulation*  
720 *Program*, *ASHRAE Journal*. 42 (2000) 49–56. doi:10.1.1.122.6852.

721 [41] *ANSI/ASHRAE/IES Standard 90.1-2016, Energy Standard for Buildings Except Low-Rise*  
722 *Residential Buildings*, (2016). isbn: 978-9990826845.

723